

**SOLUTE TRANSPORT IN THREE-DIMENSIONAL SATURATED
 POROUS MEDIA HAVING SELF-SIMILAR HYDRAULIC
 CONDUCTIVITY DISTRIBUTION¹**

Jet-Chau Wen and Chi-Ren Wang²

ABSTRACT: Customarily, it has been assumed that hydraulic conductivity is a stationary, homogeneous stochastic process with a finite variance for stochastic analysis of solute transport in the subsurface. That the distribution of hydraulic conductivity may have a fractal behavior with long range correlations was suggested from field data analyses. This motivates us to further investigate how the fractal behavior of permeability distribution impacts solute transport in porous media. This study provides longitudinal and transverse macrodispersivity coefficients and the variance of the solute concentration. Longitudinal and transverse macrodispersivity coefficients are found to depend strongly on the fractal dimension (D) of logarithmic hydraulic conductivity (logK). The longitudinal and transverse macrodispersivity coefficients are the highest when D = 1, and the values decrease monotonically to zero at D = 2. Both coefficients correspond to the characteristic length scale of the logK distribution, thus are scale dependent parameters. The ratio of the transverse to the longitudinal macrodispersivity coefficient is on the order of 10⁻¹ to 10⁻⁴. Concentration variance also decreases with the fractal dimension of logK. There is no spatial spreading of solute for D = 2, and the concentration variance reaches zero for this case.

(KEY TERMS: longitudinal and transverse macrodispersivities; stationary homogeneous stochastic process; fractal behavior; long range correlation; solute transport; hydraulic conductivity.)

Wen, Jet-Chau and Chi-Ren Wang, 2003. Solute Transport in Three-Dimensional Saturated Porous Media Having Self-Similar Hydraulic Conductivity Distribution. *J. of the American Water Resources Association (JAWRA)* 39(3):597-609.

INTRODUCTION

During the past 30 years, the stochastic approach has been used to analyze the impact of heterogeneous spatial distributions of soil and aquifer properties on flow and transport processes. Initially, the spatial correlation of soil and aquifer parameters between

numerical grid points was not considered by Freeze (1975) and Warren and Skiba (1964) in their Monte Carlo simulations of hydraulic processes. Bakr *et al.* (1978) and Gelhar and Axness (1983) considered the heterogeneous random structure of the hydraulic parameter with an exponential model having finite spatial correlation ranges. The spectral theory and the perturbation method (Gelhar, 1977) were the major tools used in those analyses.

Some field data analyses (Hewett, 1986; Ababou and Gelhar, 1989; Kemblowski and Chang, 1993) have indicated that spatial distributions of geological properties (including hydraulic conductivity) can be described using the concept of a self-similar (fractal) random process. This process is characterized by a theoretically infinite scale of correlation (self-similarity), and its semivariogram is easily scaled using a power law. The self-similar random process is, in a general sense, nonstationary (Hewett, 1986; Hough, 1989). However, over a finite volume, self-similar processes can be analyzed using the extended Wiener-Khinchine relation (Hough, 1989). The same is true for the processes whose frequency range of self-similar spectral density function is limited by a low frequency cutoff limit. In these cases, fractal processes can be treated as stationary processes.

Fractal statistics have only recently been used to investigate the spatial structure of soil and aquifer properties. Ababou and Gelhar (1989), using three vertical boreholes at the Mount Simon aquifer, estimated the vertical fractal dimension of logK to be close to 2. Hewett (1986) estimated the fractal dimension of porosity in the horizontal direction from a 30-foot sand contour of the Lloydminster Sparky Oil Pool

¹Paper No. 99022 of the *Journal of the American Water Resources Association*. **Discussions are open until December 1, 2003.**

²Respectively, Professor and Graduate Student, Department of Environmental and Safety Engineering, Research Center of Soil and Water Resources and Natural Disaster Prevention, National Yunlin University of Science and Technology, 123, Sec. 3, University Road, Touliu City, Yunlin County, Taiwan 64045, R.O.C. (E-Mail/Wen: wenjc@pine.yuntech.edu.tw).

in Alberta and found it to be close to 1.3. Kemblowski and Chang (1993) indicated that the vertical distribution of hydraulic conductivity at the Berion Site, Las Cruces, New Mexico, was characterized by a highly irregular character, with the fractal dimension varying between 1.825 and 2. The relative large magnitude of the vertical fractal dimension, $D = 1.825$, indicated that the distribution was highly random, and its increments were negatively correlated. Some theoretical analyses of transport in hierarchical media were done in the last ten years (Kemblowski and Wen, 1993; Zhan and Wheatcraft, 1996; Hassan *et al.*, 1997; Molz *et al.*, 1997; Di Federico and Neuman, 1998; Hassan *et al.*, 1998). Kemblowski and Wen (1993) assumed a fractal distribution of $\log K$ along the vertical direction (perfectly stratified aquifer). By means of the assumption, Kemblowski and Wen (1993) derived the transient and asymptotic dispersivities and concentration variance in stratified soils with fractal hydraulic distributions. They concluded: (1) the macrodispersivities were problem scale dependent in transient and asymptotic phases, and (2) concentration variance was not only fractal dimension dependent but also affected by travel distance.

Zhan and Wheatcraft (1996) derived the analytical solutions of the macrodispersivity tensor of nonreactive solute transport in isotropic (nominally) and anisotropic fractal soils. In their study, they assumed one-, two-, and three-dimensional isotropic and anisotropic fractal hydraulic conductivity distributions in porous media. However, for the isotropic porous media cases, they used the concept of the nominal isotropic fractal hydraulic conductivity distribution with a fixed variance of the hydraulic conductivity distribution. These isotropic hydraulic conductivity distributions in multidimensional spaces were different from those described by Bakr *et al.* (1978) and Yaglom (1987), who pointed out additionally that the autocovariances of hydraulic conductivity distributions in multidimensional isotropic random fields are the same as one another. Therefore, the isotropic concept of hydraulic conductivity distributions presented by Bakr *et al.* (1978) and Yaglom (1987) includes not only the fixed variances of hydraulic conductivity distributions, used in Zhan and Wheatcraft (1996), but also fixed autocovariances in multidimensional spaces. In other words, the autocovariances of isotropic random fields are independent of the direction (Yaglom, 1987). Therefore, it is clear that the isotropic concept provided by Bakr *et al.* (1978) and Yaglom (1987) is stronger than the one of Zhan and Wheatcraft (1996). In our study, we have adopted the isotropic concept of hydraulic conductivity distribution provided by Bakr *et al.* (1978) and Yaglom (1987), which can be written as

$$S_{ff}^{(3)}(k) = -\frac{1}{2\pi k} \frac{dS_{ff}^{(1)}(k)}{dk} \tag{1}$$

where $S_{ff}^{(3)}(k)$ denotes the power spectrum of hydraulic conductivity distributions in a three-dimensional space; $S_{ff}^{(1)}(k)$ denotes the power spectrum of hydraulic conductivity distributions in a one-dimensional space; and k represents the wave number.

Here, we assume that $S_{ff}^{(1)}(k)$ is known as

$$S_{ff}^{(1)}(k) = \begin{cases} S_0 |k|^{-(5-2D)} & k_0 \leq k \\ S_0 |k_0|^{-(5-2D)} & k \leq k_0 \end{cases} \tag{2}$$

where k_0 has a lower limit wave number, and D denotes the fractal dimension in the range of (1, 3), k is the wave number, and S_0 is the value of the equivalent one-dimensional spectral density at $|k| = 1$. It is worth noting that the S_0 is a function of the fractal dimension. Thus, given known $S_{ff}^{(1)}(k)$, one can derive $S_{ff}^{(3)}(k)$ as

$$S_{ff}^{(3)}(k) = \begin{cases} \frac{S_0(5-2D)}{2\pi} |k|^{-(7-2D)} & k_0 \leq k \\ 0 & k \leq k_0 \end{cases} \tag{3}$$

This power spectrum of hydraulic conductivity distribution in a three-dimensional space is different from Zhan and Wheatcraft (1996). However, when the power spectrum in Equation (3) is used to obtain the variance of the hydraulic conductivity distribution in the three-dimensional space, its variance also equals the variance obtained by the one-dimensional power spectrum in Equation (2). In other words, the results in Zhan and Wheatcraft (1996) are not truly considered as second-order stationary random field of $\log K$ distributions. Also, many researches (Hassan *et al.*, 1997; Hassan *et al.*, 1998) follow an "isotropic" fractal random field of $\log K$ distributions (Zhan and Wheatcraft, 1996) to simulate the flow and solute transport in two-dimensional saturated soils. The motivation for this investigation is to find out whether the fractal dimensions of hydraulic conductivity distribution in a true second-order stationarity might influence the process of spreading.

NONREACTIVE SOLUTE TRANSPORT WITH CONVECTION AND DISPERSION MECHANISM

The three-dimensional spectral density function of the self-similar $\log K$ distribution is given as $S_{ff} = S_0 (5 - 2D) |k|^{-(7-2D)}/(2\pi)$. It is clear that the spectral

density function S_{ff} has a singular point at the origin because $S_{ff}(k) \rightarrow \infty$ when $k \rightarrow 0$. Since k is inversely proportional to the characteristic length (L) of the domain site, this implies that the domain scale of a porous medium is infinite (Kemblowski and Wen, 1993; Zhan and Wheatcraft, 1996; Hassan *et al.*, 1998). However, as real field scenarios usually have some maximum length constraints on the subsurface system, there exists a maximum characteristic length scale (minimum k) beyond which the spectrum S_{ff} can be truncated. This idea is to allow the lower limit of the wave number to be inversely proportional to the characteristic length of the domain of interest (Ababou and Gelhar, 1989; Kemblowski and Chang, 1993; Kemblowski and Wen, 1993; Hassan *et al.*, 1998). In the study, the lower limit of the wave number is the characteristic cutoff frequency k_0 and can be expressed in terms of the associated characteristic length scale, L ,

$$k_0 = \frac{2\pi}{L} \tag{4}$$

The physical meaning of L is related to the contaminant plume dimension that is transported in saturated soils or aquifers.

The governing equation for steady state nonreactive solute transport with convection and pore level dispersion is given as

$$\frac{\partial(q_i c)}{\partial x_i} = \frac{\partial}{\partial x_i} \left[E_{ij} \frac{\partial c}{\partial x_j} \right] \tag{5}$$

where c is the concentration of solute transport; q_i is the specific discharge in the x_i direction; E_{ij} is the local bulk dispersion coefficient, equal to nD_{ij} ; n is the porosity; and D_{ij} is the pore level dispersion coefficient tensor (including hydrodynamic dispersion and molecular diffusion).

The small perturbation method is applied to derive the stochastic differential equations for flow and concentration. The Fourier-Stieltjes representation for perturbed quantities (Gelhar and Axness, 1983) is used to transform the perturbation equation into the frequency domain. Consequently, all the spectral density functions needed to evaluate the mean parameters of the flow and solute transport processes are derived. Following the procedures presented in Gelhar and Axness (1983), the diagonal elements of macrodispersivity, A_{ii} , are given as

$$A_{ii} = \int_{-\infty}^{\infty} \frac{\left(\delta_{i1} - \frac{k_1 k_i}{k^2} \right)^2 \left[\alpha_L k_1^2 + \alpha_T (k_2^2 + k_3^2) \right] S_{ff}(\vec{k}) d\vec{k}}{\gamma^2 \left\{ k_1^2 + \left[\alpha_L k_1^2 + \alpha_T (k_2^2 + k_3^2) \right]^2 \right\}} \tag{6}$$

$i = 1, 2, 3$

where α_L and α_T represent the pore level longitudinal and transverse dispersivity coefficients (assumed to be equal), γ represents the ratio of the mean specific discharge to the geometric mean of hydraulic conductivity as well as the mean hydraulic gradient in the major flow direction, and δ_{i1} represents the Kronecker delta. The nondiagonal elements of macrodispersivity, A_{ij} where $i \neq j$, are equal to 0 (Gelhar and Axness, 1983).

Using the Fourier-Stieltjes representations of specific discharge and solute concentration in the differential equation of solute transport (Equation 5), the following expression can be obtained.

$$\left[ik_1 + \alpha_L k_1^2 + \alpha_T (k_2^2 + k_3^2) \right] q dZ_c(\vec{k}) = G_j dZ_{qj}(\vec{k}) \tag{7}$$

where q is the mean specific discharge, G_j denotes the gradient of mean solute concentration in the j direction ($\partial \bar{c} / \partial x_j$), the $dZ_c(\vec{k})$ represents the generalized amplitude of the solute concentration, and the $dZ_{qj}(\vec{k})$ is the generalized amplitude of specific discharge in the j direction. Since the generalized amplitude of specific discharge is known as $dZ_{qj}(\vec{k}) = K_G$

$\left[J_j - \frac{J_m k_m k_j}{k^2} \right] dZ_f(\vec{k})$ (Gelhar and Axness, 1983), substituting it for the generalized amplitude of specific discharge in the last identity gives the following.

$$dZ_c(\vec{k}) = \frac{G_j K_G}{q} \frac{\left[J_j - \frac{J_m k_m k_j}{k^2} \right]}{\left[ik_1 + \alpha_L k_1^2 + \alpha_T (k_2^2 + k_3^2) \right]} dZ_f(\vec{k}) \tag{8}$$

where J_j or J_m represents the mean hydraulic gradient in the j direction or m direction, respectively. The last equation is known as the formula of the generalized amplitude of the solute concentration. The complex conjugate of the last equation is

$$dZ_c^*(\vec{k}) = \frac{G_j K_G}{q} \frac{\left[J_j - \frac{J_m k_m k_j}{k^2} \right]}{\left[-ik_1 + \alpha_L k_1^2 + \alpha_T (k_2^2 + k_3^2) \right]} dZ_f^*(\vec{k}) \tag{9}$$

Multiplying the last equation with the formula of generalized amplitude of the solute concentration yields

$$dZ_c(\bar{k})dZ_c^*(\bar{k}) = \frac{G_i G_j K_G^2}{q^2} \frac{\left[J_i - \frac{J_m k_m k_i}{k^2} \right] \left[J_j - \frac{J_m k_m k_j}{k^2} \right]}{\left\{ k_1^2 + \left[\alpha_L k_1^2 + \alpha_T (k_2^2 + k_3^2) \right]^2 \right\}} dZ_f(\bar{k})dZ_f^*(\bar{k}) \tag{10}$$

Taking the expectation of the last identity and applying the spectral representation theorem, the spectral density function of solute concentration can be obtained as

$$S_{cc}(\bar{k}) = \frac{G_i G_j K_G^2}{q^2} \frac{\left[J_i - \frac{J_m k_m k_i}{k^2} \right] \left[J_j - \frac{J_m k_m k_j}{k^2} \right]}{\left\{ k_1^2 + \left[\alpha_L k_1^2 + \alpha_T (k_2^2 + k_3^2) \right]^2 \right\}} S_{ff}(\bar{k}) \tag{11}$$

Since this spectral density function of solute concentration is related to the mean concentration gradients (G_1 , G_2 , and G_3), the mean specific discharge (q), and the mean hydraulic gradient in the major flow direction (J_1), it is difficult to analyze the concentration variance with the spectral density function. To analyze the concentration variance with the spectral density function, we simplify the formula by considering the mean concentration gradient to be significant only in the major flow direction. This may lose some of the physical detail of solute transport in saturated soils with self-similar logK distribution. However, the basic physical behavior of solute transport in heterogeneous soils or aquifers still can be seen from the simplification. Therefore, the last equation can be simplified as

$$S_{cc}(\bar{k}) = \frac{G_1^2 K_G^2 J_1^2 \left[1 - \frac{k_1^2}{k^2} + \frac{k_1^4}{k^4} \right] S_{ff}(\bar{k})}{q^2 \left\{ k_1^2 + \left[\alpha_L k_1^2 + \alpha_T (k_2^2 + k_3^2) \right]^2 \right\}} \tag{12}$$

The last equation is known as a simplified spectral density function of solute concentration. Since γ in Equation (6) is the ratio of the mean specific discharge to the geometric mean of hydraulic conductivity as well as the mean hydraulic gradient in the major flow direction, it is defined as

$$\gamma = \frac{q}{K_G J_1} \tag{13}$$

Substituting the last equation for the simplified spectral density function of solute concentration yields

$$S_{cc} = \frac{G_1^2 S_{ff} \left[1 - 2 \frac{k_1^2}{k^2} + \frac{k_1^4}{k^4} \right]}{\gamma^2 \left\{ k_1^2 + \left[\alpha_L k_1^2 + \alpha_T (k_2^2 + k_3^2) \right]^2 \right\}} \tag{14}$$

All the notations in Equation (14) are the same as those used in Equation (6).

MACRODISPERSIVITY COEFFICIENTS AND CONCENTRATION VARIANCE

Integrating Equation (6) yields the formulas for asymptotic longitudinal and transverse macrodispersivity coefficients.

Longitudinal Macrodispersivity (A₁₁)

$$\begin{aligned}
 A_{11} = & \frac{\sigma_f^2 \alpha_L}{\gamma^2} \left[\frac{(4-2D)X}{(5-2D)} \tan^{-1}(X) - \frac{(4-2D)X^2}{(5-2D)(6-2D)} {}_2F_1(1, 3-D, 4-D, -X^2) - 2 + \frac{(4-2D)}{(3-2D)X} \tan^{-1}(X) \right. \\
 & - \frac{2}{(3-2D)} {}_2F_1(1, 2-D, 3-D, -X^2) + \frac{1}{3} - \frac{(4-2D)}{(2-2D)X^2} + \frac{(4-2D)}{(1-2D)X^3} \tan^{-1}(X) \\
 & \left. - \frac{(4-2D)}{(1-2D)(2-2D)X^2(1+X^2)} - \frac{2}{(1-2D)(2-2D)} {}_2F_1(2, 2-D, 3-D, -X^2) \right] \tag{15}
 \end{aligned}$$

where ${}_2F_1(\alpha, \beta, \gamma, z)$ is the hypergeometric function (Gradshteyn and Ryzhik, 1980), $X = L/(2\pi\alpha_L)$, and σ_f^2 is the variance of logK. The variance of logK can be estimated from its power spectrum by using the Wiener-Khintchine relation with zero separation distance. The result can be expressed as

$$\sigma_f^2 = \frac{2S_0(5-2D)}{(4-2D)} \left(\frac{2\pi}{L} \right)^{-(4-2D)} \tag{16}$$

Equation (15) can be simplified further by assuming that the pore level dispersivity is much smaller than the associated characteristic length scale, $2\pi\alpha_L \ll L$. This yields

$$A_{11} = \frac{\sigma_f^2 \alpha_L}{\gamma^2} \frac{(4-2D)X}{(5-2D)} \frac{\pi}{2} = \frac{\sigma_f^2(4-2D)}{\gamma^2(5-2D)} \left(\frac{L}{4} \right) \tag{17}$$

Equation (17) shows that the longitudinal macrodispersivity is related to the characteristic length scale, the fractal dimension D, and the variance of logK.

Transverse Macrodispersivity (A₂₂)

$$\begin{aligned}
 A_{22} = & \frac{\sigma_f^2 \alpha_L}{\gamma^2} \left[\frac{1}{3} + \frac{(4-2D)}{2(2-2D)X^2} - \frac{(4-2D) \tan^{-1}(X)}{2(1-2D)X^3} - \frac{(4-2D) \tan^{-1}(X)}{2(3-2D)X} + \frac{(4-2D)}{2(1-2D)(2-2D)X^2(1+X^2)} \right. \\
 & \left. + \frac{{}_2F_1(2, 2-D, 3-D, -X^2)}{(1-2D)(2-2D)} + \frac{{}_2F_1(1, 2-D, 3-D, -X^2)}{2(3-2D)} \right] \tag{18}
 \end{aligned}$$

Equation (18) can be simplified further by assuming that $2\pi\alpha_L \ll L$ to obtain

$$A_{22} = \begin{cases} \frac{\sigma_f^2 \alpha_L}{3\gamma^2} & D \neq 2 \\ 0 & D = 2 \end{cases} \tag{19}$$

This equation is the same as the expression derived by Gelhar and Axness (1983), who applied the exponential covariance structure of logK distribution for investigating the solute transport in the subsurface, except for the case when D = 2. Again, it can be seen that the solute transport in the exponential covariance structure of the logK field has a dominant spreading process. Therefore, a constant transverse macrodispersivity is reached asymptotically. However, in the fractal logK field, there are spreading and mixing processes. The spreading process is strong when the fractal dimension of the logK field is small. The mixing process is strong when the fractal dimension of the logK field is large. However, a constant transverse macrodispersivity is also reached asymptotically no matter what the fractal dimension is. Finally, the transverse macrodispersivity is equal to zero at D = 2 because the solute transport is fully mixed in the subsurface of the fractal logK field.

Concentration Variance (σ_{cc}^2)

By integrating the concentration spectral density function (Equation 14), the concentration variance is estimated as

$$\sigma_{cc}^2 = \frac{G_1^2 \sigma_f^2 \alpha_L^2}{\gamma^2} \left[\frac{(4-2D)X^3}{(7-2D)} \tan^{-1}(X) - \frac{(4-2D)X^4}{(7-2D)(8-2D)} {}_2F_1(1, 4-D, 5-D, -X^2) - \frac{2(4-2D)X^2}{(6-2D)} + \frac{2(4-2D)X \tan^{-1}(X)}{(5-2D)} \right. \\ \left. - \frac{2(4-2D)X^2}{{(5-2D)(6-2D)}} {}_2F_1(1, 3-D, 4-D, -X^2) + \frac{(4-2D)X^2}{3(6-2D)} - 1 + \frac{(4-2D)}{(3-2D)X} \tan^{-1}(X) - \frac{{}_2F_1(1, 2-D, 3-D, -X^2)}{(3-2D)} \right] \tag{20}$$

Assuming $2\pi\alpha_L \ll L$, a simplified expression is obtained as follows:

$$S_0 = \frac{(4-2D)\sigma_f^2}{2(5-2D)} \left(\frac{2\lambda}{L} \right)^{(4-2D)} \tag{22}$$

$$\sigma_{cc}^2 = \frac{G_1^2 \sigma_f^2 \alpha_L^2}{\gamma^2} \frac{(4-2D)X^3}{(7-2D)} \frac{\pi}{2} = \frac{G_1^2 \sigma_f^2}{\gamma^2 \alpha_L} \frac{(4-2D)}{(7-2D)} \frac{\pi}{2} \left(\frac{L}{2\pi} \right)^3 \tag{21}$$

Again, we can see that the variance is equal to zero for $D = 2$ because the solute transport process is fully mixed in the subsurface. This result is consistent with the results of longitudinal and transverse macrodispersivities (Equations 17 and 18).

ANALYSIS OF THE BEHAVIOR OF SOLUTE TRANSPORT PARAMETERS

The relationships among the three transport parameters (longitudinal and transverse macrodispersivity coefficients and concentration variance) and two principal characteristics of the logK distribution (the fractal dimension D and the length scale L) will be investigated. To properly evaluate the impact of the characteristic length scale on the transport parameters, the variance of logK (which is a scale dependent property) has to be expressed in terms of the length scale L (Equation 16). This behavior is analyzed by maintaining a constant fractal dimension.

However, to study the impact of the fractal dimension on transport parameters, it is not appropriate to express the variance of logK using Equation (16). The reason is that the character of S_0 is not clear in Equation (16). Thus, Equation (16) can be rewritten as

Equation (22) shows that S_0 is dependent upon the fractal dimension. Therefore, we cannot use Equation (16) directly to examine the impact of the fractal dimension on transport parameters, because if S_0 is constant, then the fractal dimension has to be constant. However, if the fractal dimension changes, S_0 also changes, which may or may not cause the logK variance to change. For instance, in a real scenario, there may be many different saturated soils or aquifers that have the same variance of logK with a constant length scale L , even though their fractal dimensions and S_0 s are different. Therefore, we cannot investigate the impact of the fractal dimension on the transport parameters with constant L only. Thus, to study the impact of the fractal dimension on transport parameters, constant characteristic length, L , is assumed, and therefore constant variance of logK is also assumed.

To investigate the scale dependence of longitudinal macrodispersivity under the same fractal dimension, the behavior of a normalized macrodispersivity is examined and represented below.

$$\bar{A}_{11} = \frac{A_{11}(X, D)}{A_{11}(X = 1000, D)} \tag{23}$$

Figure 1 depicts the behavior of this normalized macrodispersivity as a fixed fractal dimension. From Figure 1 a general statement can be made that, for each fixed fractal dimension, the larger the characteristic length scale, the higher the macrodispersivity. The larger characteristic length scale means a more heterogeneous logK, which results in an increased

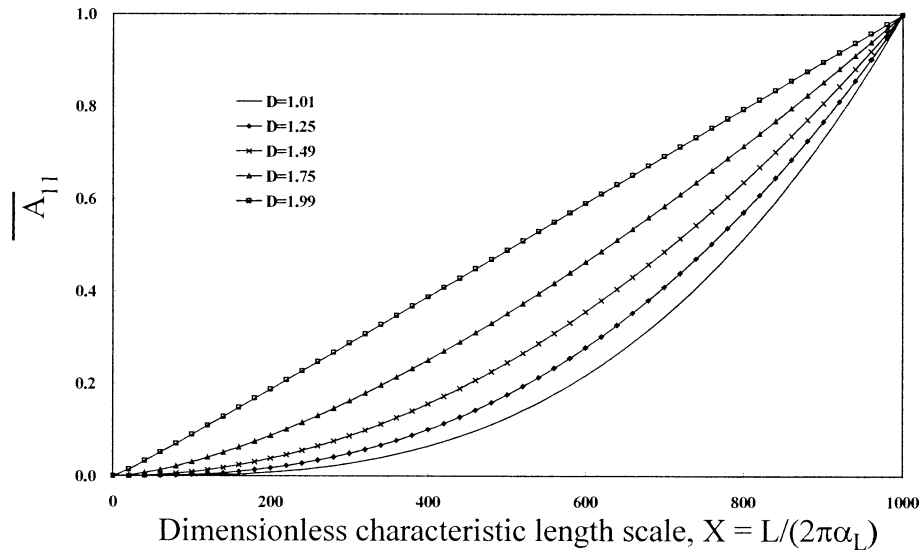


Figure 1. Normalized Longitudinal Macrodispersivity (Equation 23).

variance in logK. Consequently, the longitudinal macrodispersivity is proportional to the variance of logK (see Equation 15).

To investigate the impact of the fractal dimension on the longitudinal macrodispersivity under the same characteristic length scale, Equation (15) is normalized, assuming a constant variance of logK.

$$\tilde{A}_{11} = \frac{A_{11}(X, D)}{A_{11}(X, D \rightarrow 1)} \tag{24}$$

The behavior of this quantity as a function of D for each fixed characteristic length is depicted in Figure 2. It is clear from this figure that the fractal dimension plays an important role in the process of solute spreading in porous media. The longitudinal macrodispersivity is largest for D = 1, and decreases monotonically to zero at D = 2. This behavior is related to the structure of the velocity field, which in turn is related to the logK distribution. The increasing fractal dimension of a random process results in the change of correlation between the increments of

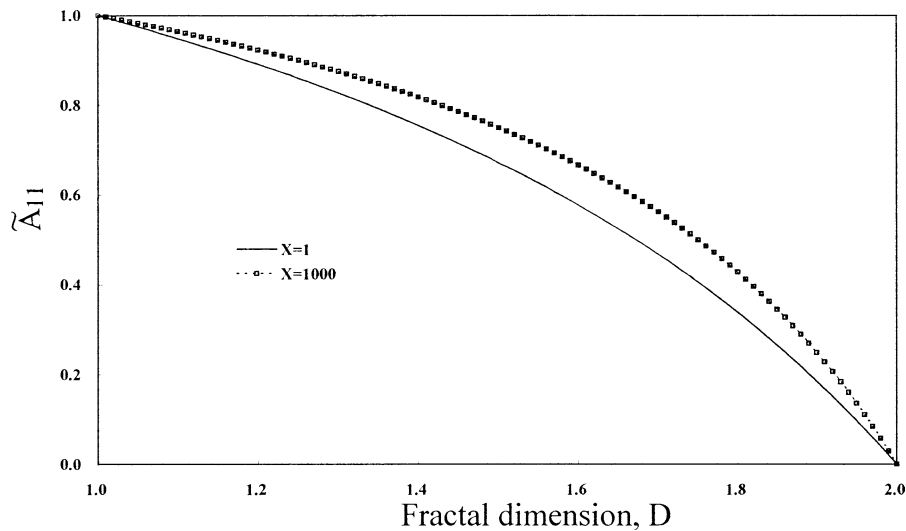


Figure 2. Normalized Longitudinal Macrodispersivity (Equation 24).

this process. In particular, for D less than 1.5, the increments are positively correlated; whereas for D greater than 1.5, they are negatively correlated. The larger the negative correlation of logK increments, the “noisier” the velocity field. In such a field the local spreading caused by a heterogeneous velocity field could be overcome easily by the negative correlation in the velocity increments, which in turn results in a smaller magnitude of plume spreading.

Figure 3 shows the ratio of an exactly estimated longitudinal macrodispersivity (Equation 15) to its approximation (Equation 17). It is clear that for X = 1,000 the approximation is very close to the exact solution.

To investigate the scale dependence of the transverse macrodispersivity, the following expression for normalized transverse macrodispersivity is used.

$$\bar{A}_{22} = \frac{A_{22}(X, D)}{A_{22}(X = 1000, D)} \tag{25}$$

Figure 4 shows that the nature of the transverse macrodispersivity is similar to that of the longitudinal macrodispersivity in the sense that both are proportional to the characteristic length scale L.

To investigate the impact of the fractal dimension of permeability distribution on transverse macrodispersivity, the following normalized macrodispersivity is used.

$$\tilde{A}_{22} = \frac{A_{22}(X, D)}{A_{22}(X, D \rightarrow 1)} \tag{26}$$

Figure 5 shows the impact of the fractal dimension on transverse macrodispersivity. As can be seen from this figure, transverse macrodispersivity decreases as the fractal dimension increases. It is believed that the physical explanation of this behavior is the same as that for the longitudinal macrodispersivity.

The ratio of an exactly estimated transverse macrodispersivity (Equation 18) to its approximation (Equation 19) is shown in Figure 6 for the dimensionless characteristic length scale ranging from 10³ to 10¹⁰. The ratio is close to 1 for the fractal dimension less than 1.5. For the fractal dimension greater than 1.5, the approximate solution is inaccurate for X less than 10³. Even for X = 10⁹, the approximate solution is not correct for D greater than 1.8. It is, therefore, clear that one has to be careful when using the approximate solution, particularly for relatively small characteristic length scales. On the other hand, the approximate solution can be used as the upper bound for transverse macrodispersivity.

The ratio of the exact solutions of the transverse macrodispersivity (Equation 18) to longitudinal macrodispersivity (Equation 15) is also examined (Figure 7). For a constant characteristic length scale, the transverse macrodispersivity is always smaller than the longitudinal macrodispersivity. This occurs because the variance of the velocity field is smaller in the transverse direction than that in the mean flow direction, thus resulting in less spreading in the transverse direction.

To analyze the relationship between the concentration variance and the characteristic length scale, a normalized concentration variance is given as

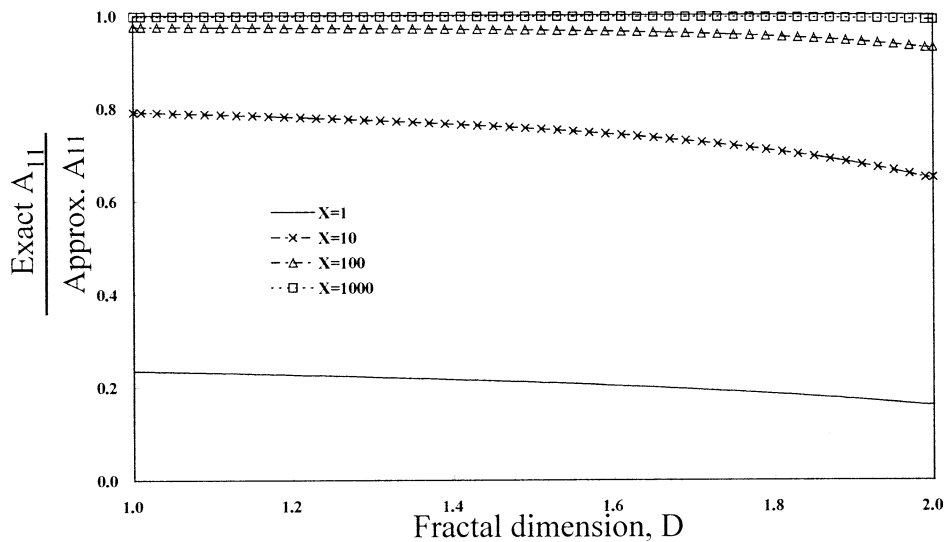


Figure 3. The Ratio of Exact and Approximate Longitudinal Dispersivity Coefficients.

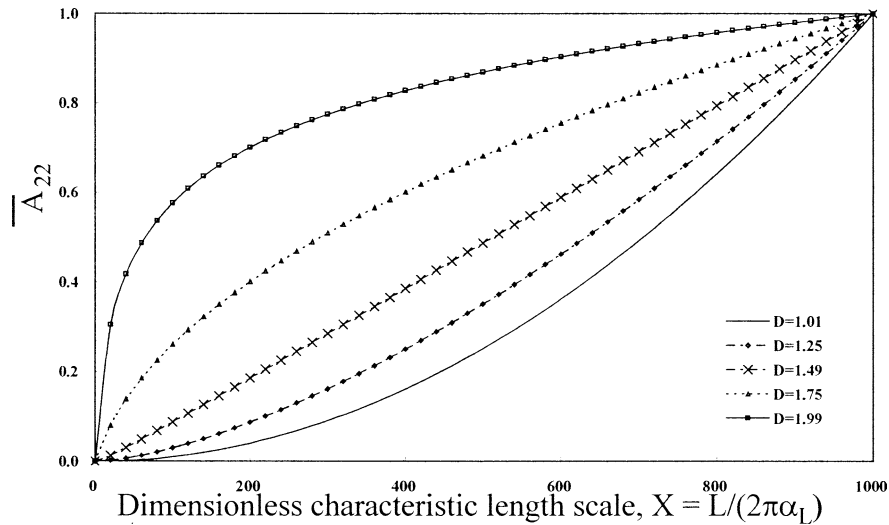


Figure 4. Normalized Transverse Macrodispersivity (Equation 25).

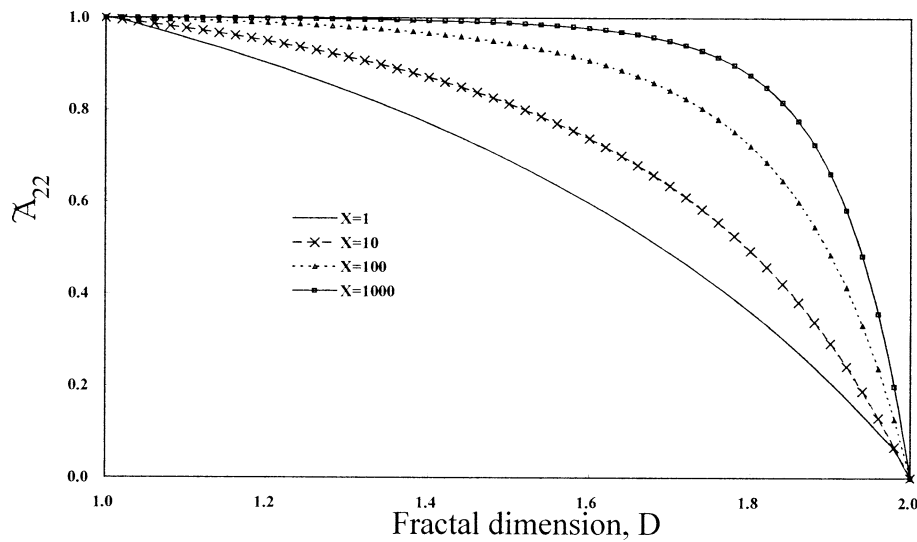


Figure 5. Normalized Transverse Macrodispersivity (Equation 26).

$$\bar{\sigma}_{cc}^2 = \frac{\sigma_{cc}^2(X, D)}{\sigma_{cc}^2(X = 1000, D)} \tag{27}$$

$$\tilde{\sigma}_{cc}^2 = \frac{\sigma_{cc}^2(X, D)}{\sigma_{cc}^2(X, D \rightarrow 1)} \tag{28}$$

Figure 8 shows that the concentration variance increases with an increase in the characteristic length scale. This behavior is similar to that of the longitudinal macrodispersivity.

Another form of normalized concentration variance used to investigate the impact of the fractal dimension on concentration fluctuations is shown below.

In Figure 9, the behavior of this normalized variance of solute concentration (Equation 28) is illustrated. The concentration variance decreases when the fractal dimension increases. This behavior is also similar to that of the longitudinal macrodispersivity.

Finally, the range of applicability of the approximate formula for concentration variance (Equation 21) is investigated. The ratio of the exact solution

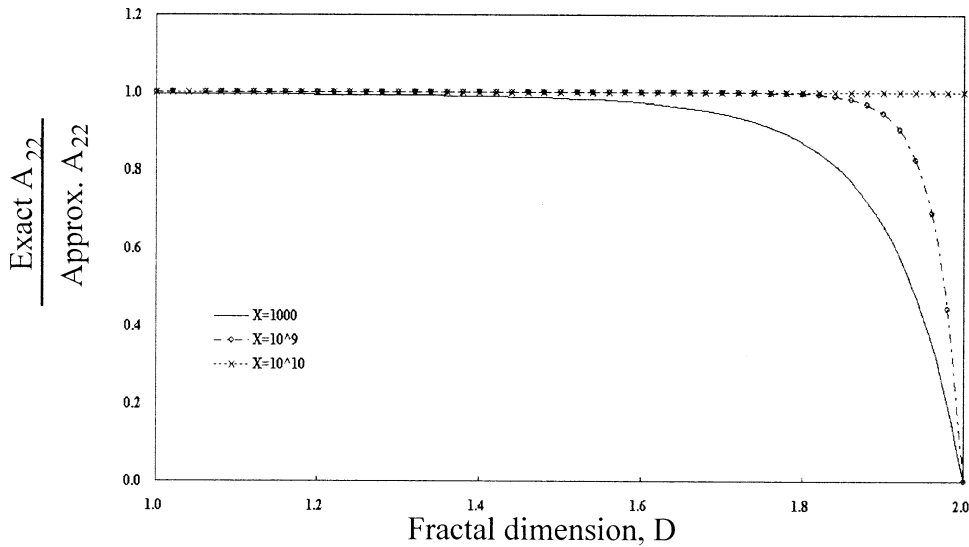


Figure 6. The Ratio of Exact and Approximate Transverse Dispersivity Coefficients.

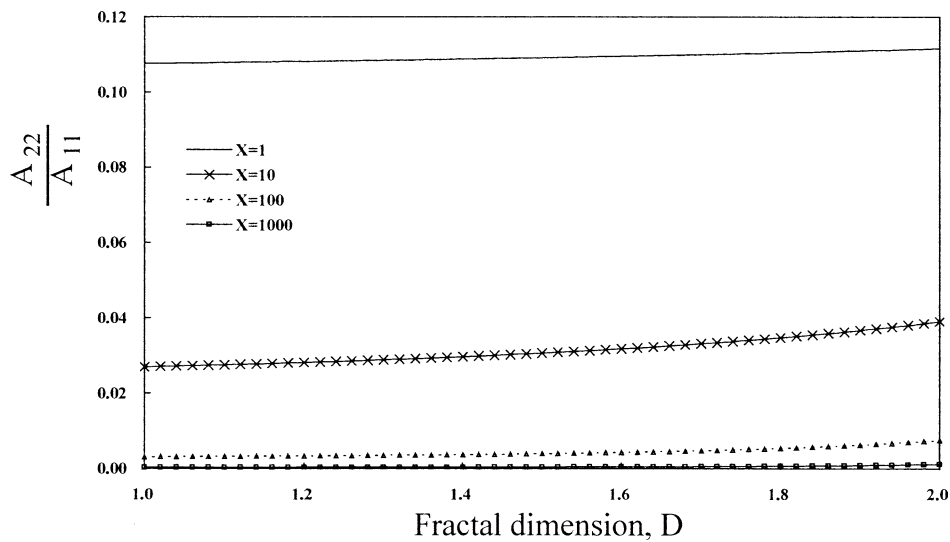


Figure 7. Ratio of Transverse to Longitudinal Dispersivity Coefficients.

(Equation 20) to the approximate one (Equation 28) is shown in Figure 10. It can be seen that the approximate solution is valid when the characteristic length scale, X , is larger than 1,000.

SUMMARY

It has been shown that the fractal dimension and the characteristic length scale of $\log K$ play an important role in the macrodispersivity and concentration

variance solute transport process. Longitudinal and transverse macrodispersivity coefficients (or, more precisely, longitudinal and transverse spreading coefficients) depend strongly on the fractal dimension of $\log K$. The highest values of longitudinal and transverse macrodispersivity occur for $D = 1$, and they decrease monotonically to zero at $D = 2$. This behavior is related to the structure of the velocity field, which in turn is related to the $\log K$ distribution. The increasing fractal dimension of a random process results in the change of correlation between the increments of this process. In particular, for D less than

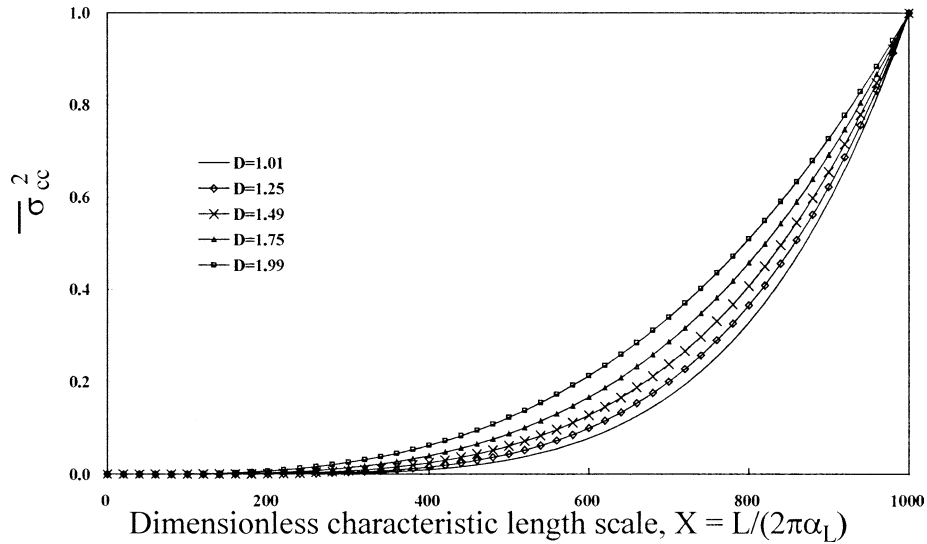


Figure 8. Normalized Variance of Concentration (Equation 27).

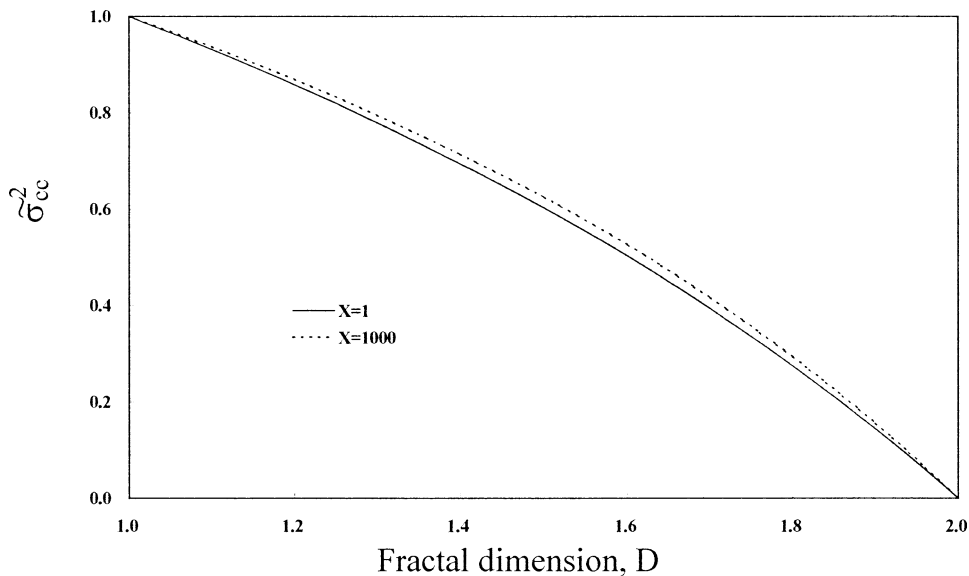


Figure 9. Normalized Variance of Concentration (Equation 28).

and equal to 1.5, the increments are positively correlated; whereas for D greater than and equal to 1.5, they are negatively correlated (Voss, 1985a,b, 1986). The larger the negative correlation of $\log K$ increments, the “noisier” the velocity field. In such a field, the spreading caused by a heterogeneous velocity field could be overcome easily by the negative correlation in the velocity increments, which in turn results in a smaller magnitude of plume spreading. This “smoothing” process is further enhanced by pore level mixing. The longitudinal and transverse spreading

coefficients are found to be scale-dependent parameters, since they depend on the characteristic length scale of $\log K$. The ratio of longitudinal and transverse spreading coefficients is on the order of 10^1 to 10^4 .

Concentration variance, for reasons similar to the ones discussed above, also decreases with the increase in fractal dimension of $\log K$. For $D = 2$, no spatial spreading of solute took place, and therefore the variance about the mean concentration field was equal to zero.

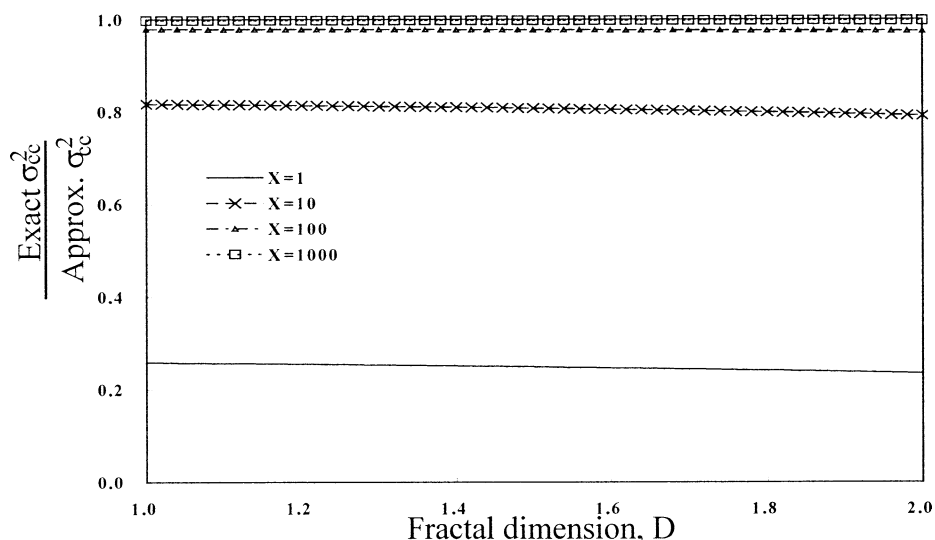


Figure 10. The Ratio of Exact to Approximate Concentration Variances.

The scale effect on the spreading characteristics of solute in the longitudinal and transverse direction has different increments. The increments of normalized longitudinal macrodispersivity had fewer increments during the small dimensionless characteristic length scale than that of normalized transverse macrodispersivity. This was explained by using the positive correlation scale of specific discharge, which was found in Ababou (1988). Since the positive correlation scale of specific discharge in the lateral direction is larger than the scale in the longitudinal direction, this creates a strong tendency for solute to spread in the transverse direction. Consequently, the quantities of normalized A_{22} are higher than those of normalized A_{11} .

The fractal dimension of permeability influences the different spreading behaviors of solute in the longitudinal and transverse directions. Since the variance of specific discharge in the mean flow direction is larger than the one in the lateral direction, the pore level mixing is enhanced in the mean flow direction. Consequently, the normalized A_{11} decreases more quickly than that of normalized A_{22} . However, both spreading coefficients, A_{11} and A_{22} , became zero when D approached 2, and the normalized A_{22} decreases quickly when D approached 2.

The longitudinal macrodispersivity is significantly larger than the transverse one, and the ratio increases with the normalized characteristic self-similarity scale and the fractal dimension.

When the normalized characteristic length scale, $L/(2\pi\alpha_L)$, is larger than 1,000, the approximate solutions for the longitudinal macrodispersivity and concentration variance are close to the exact ones. This is

not true for the transverse dispersivity. The approximate solution for this parameter is quite different from the exact one, even for $X = 10^9$, and particularly for D greater than 1.8.

The fractal behavior of permeability distribution strongly impacts the solute transport process in the subsurface. In addition, the solute transport process is influenced by the characteristic length scale of $\log K$. The application of these two findings will be examined in a forthcoming paper by using the finite volume method to predict the Borden site data (Sudicky, 1986).

ACKNOWLEDGMENTS

This work was sponsored by the National Science Council under Grants NSC 89-2218-E-224-029 and NSC 90-2211-E-224-018. The authors would like to acknowledge Ms. Resta L. Saphore-Cheng for her help in proofreading this paper.

LITERATURE CITED

- Ababou, R., 1988. Three-Dimensional Flow in Random Porous Media. Ph.D. dissertation, Massachusetts Institute of Technology, Boston, Massachusetts.
- Ababou, R. and L. W. Gelhar, 1989. Self-Similar Randomness and Spectral Conditioning: Analysis of Scale Effects in Subsurface Hydrology. *In: Dynamics of Fluids in Hierarchical Porous Formations*, J. H. Cushman (Editor). Academic Press Ltd., London, England, pp. 393-428.
- Bakr, A. A., L. W. Gelhar, A. L. Gutjahr, and J. R. MacMillan, 1978. Stochastic Analysis of Spatial Variability in Subsurface Flows. 1. Comparison of One- and Three-Dimensional Flows. *Water Resour. Res.* 14(2):263-271.

- Di Federico V. and S. P. Neuman, 1998. Transport in Multiscale Log Conductivity Fields with Truncated Power Variograms. *Water Resour. Res.* 34(5):963-973.
- Freeze, R. A., 1975. A Stochastic-Conceptual Analysis of One-Dimensional Groundwater Flow in Nonuniform Homogeneous Media. *Water Resour. Res.* 11(5):725-741.
- Gelhar, L. W., 1977. Effects of Hydraulic Conductivity Variations on Groundwater Flows. *In: Hydraulic Problems Solved by Stochastic Methods.* Water Resources Publications, Fort Collins, Colorado, pp. 409-429.
- Gelhar, L. W. and C. L. Axness, 1983. Three-Dimensional Stochastic Analysis of Macrodispersion in Aquifers. *Water Resour. Res.* 19(1):161-180.
- Gradshteyn, I. S. and I. M. Ryzhik, 1980. Table of Integrals, Series, and Products. Academic Press Inc., Orlando, Florida.
- Hassan, A. E., J. H. Cushman, and J. W. Delleur, 1997. Monte Carlo Studies of Flow and Transport in Fractal Conductivity Fields: Comparison With Stochastic Perturbation Theory. *Water Resour. Res.* 33(11):2519-2534.
- Hassan A. E., J. H. Cushman, and J. W. Delleur, 1998. A Monte Carlo Assessment of Eulerian Flow and Transport Perturbation Models. *Water Resour. Res.* 34(5):1143-1163.
- Hewett, T. A., 1986. Fractal Distributions of Reservoir Heterogeneity and Their Influence on Fluid Transport. Annual Conference and Exhibition of the Society Petroleum Engineering, New Orleans, Louisiana, SPE 15386.
- Hough, S. E., 1989. On the Use of Spectral Methods for the Determination of Fractal Dimension. *Geophysical Research Letters* 16(7):673-676.
- Kemblowski, M. W. and C-M Chang, 1993. Infiltration in Soils With Fractal Permeability Distribution. *Ground Water* 31:187-192.
- Kemblowski, M. W. and J. C. Wen, 1993. Contaminant Spreading in Stratified Soils With Fractal Permeability Distribution. *Water Resour. Res.* 29(2):419-425.
- Molz, F. J., H. H. Liu, and J. Szulga, 1997. Fractional Brownian Motion and Fractional Gaussian Noise in Subsurface Hydrology: A Review, Presentation of Fundamental Properties, and Extensions. *Water Resour. Res.* 33(10):2273-2286.
- Sudicky, E.A., 1986. A Natural Gradient Experiment on Solute Transport in a Sand Aquifer: Spatial Variance of Hydraulic Conductivity and Its Role in the Dispersion Process. *Water Resour. Res.* 22(13):2069-2082.
- Voss, R. F., 1985a. Fundamental Algorithms for Computer Graphics. *In: NATO ASI Series, F17, R. A. Earnshaw (Editor).* Springer-Verlag, Berlin Heidelberg, Germany, pp. 805-835.
- Voss, R. F., 1985b. Random Fractals: Characterization and Measurement. *In: Scaling Phenomena in Disordered Systems, R. Pynn and A. Skjeltorp (Editor).* Plenum Publishing Corporation, New York, New York, pp. 37-48.
- Voss, R. F., 1986. Characterization and Measurement of Random Fractals. *Physica Scripta.* T13:27-32.
- Warren, J. E. and F. F. Skiba, 1964. Macroscopic Dispersion. *Transactions of American Institute of Mining, Metallurgical, and Petroleum Engineers* 231:215-230.
- Yaglom, A. M., 1987. Correlation Theory of Stationary and Related Random Functions I Basic Results. Springer-Verlag, New York, New York.
- Zhan, H. and S. W. Wheatcraft, 1996. Macrodispersivity Tensor for Nonreactive Solute Transport in Insotropic and Anisotropic Fractal Porous Media: Analytical Solutions. *Water Resour. Res.* 32(12):3461-3474.